

*OBSERVATION OF COMPLEX SINGULARITIES OF DIRECT NUCLEAR REACTION
AMPLITUDES*

É. I. DUBOVOÏ and I. S. SHAPIRO

Institute of Theoretical and Experimental Physics, Moscow Physico-technical Institute

Submitted to JETP editor May 16, 1966

J. Exptl. Theoret. Phys. (U.S.S.R.) 51, 1251–1259 (October, 1966)

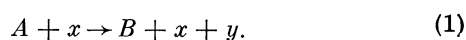
Cross sections for direct reactions of the type $A(x, xy)B$ are investigated as functions of the transferred momentum and the kinetic energy of the emitted particles near a moving complex singularity with respect to these variables. The possibility of utilizing normal threshold singularities of triangular diagrams for identifying the mechanism of the reaction is noted. Analytic formulas are obtained for the differential cross section and contour maps are given of the surface corresponding to this cross section.

1. INTRODUCTION

ACCORDING to present ideas a direct process reduces to reactions occurring between an incident particle and virtual particles. The number of virtual particles, the values of their masses and also the type of virtual reactions determine the mechanism of the process which in an essential manner affects the dependence of the amplitude on the kinematic variables, or, in other words, the position and nature of the singularities of the amplitude with respect to these variables (cf. [1]). It is clear that it is desirable to conduct the experimental investigation of a direct reaction undertaken in order to ascertain its mechanism, over a range of values of the kinematic variables which is situated as closely as possible to the expected singularities.

As a rule, the amplitudes for direct reactions of binary type (two particles in the final state) have singularities with respect to the transferred momentum which occur at real negative values. These singularities are situated fairly close to the boundary of the physical region for reactions of deuteron stripping and pickup. In other cases the singularities lie considerably further, and as a result of this the dependence to which they give rise of the differential cross section on the transferred momentum is much less pronounced. Because of this it often turns out to be difficult to identify the mechanism of the reaction by measuring angular distributions.

An essentially different situation occurs for reactions with the production of three particles, in particular for processes of the type



It turns out that in this case new possibilities arise for establishing the mechanism of the reaction by studying the dependence of its amplitude on two variables—the energy ω of the particles in their c.m.s. and the transferred momentum $q = |\mathbf{p}_x - \mathbf{p}'_x|$, where \mathbf{p}_x and \mathbf{p}'_x are the momenta of particle x before and after the reaction. The new features compared with binary reactions are in this case, first of all, the motion of the singularities, i.e., the change in the position of a singularity with respect to one of the variables (for example, with respect to ω) depending on the value of the other variable (q) and, secondly, the fact that these singularities can be complex.

If ω_Δ and q_Δ are complex singularities with respect to the variables ω and q , then $\text{Re } \omega_\Delta$ and $\text{Re } q_\Delta$ are numbers lying within the range of physical values of the variables ω and q . If, moreover, $\text{Im } \omega_\Delta$ and $\text{Im } q_\Delta$ are sufficiently small (this condition is made more precise later), then the singularities will be situated close to the physical region similarly to the situation which exists in the case of a Breit-Wigner resonance level. Then for values of ω lying in the neighborhood of $\text{Re } \omega_\Delta$ irregularities appear in the dependence of the differential cross section on ω the position and shape of which will depend on the transferred momentum q . Assuming a definite mechanism for the direct process (1) one can theoretically calculate the function $\omega_\Delta(q)$ and the behavior of the differential cross section $\partial^2 \sigma / \partial \omega \partial q^2$ near the singularities.

The aim of the present paper is to derive appropriate formulas and also to obtain graphical material suitable for comparison with experimental data.

The problem of the position of complex singularities of nonrelativistic diagrams was first considered by Blokhintsev, Dolinskiĭ, and Popov.^[2] Later Valuev^[3] and Anisovich and Dakhno^[4] calculated the behavior of the cross section near the singularity for the reaction $N + \pi \rightarrow N + 2\pi$ and Dal'karov^[5] calculated it for the reaction $p + d \rightarrow p + X$. Our results, as applied to direct nuclear reactions, differ from^[3-5] by a greater degree of generality (the formulas given below and the numerical results are valid for all nonrelativistic reactions of type (1)) and by a complete investigation of the surface $\partial^2\sigma(\omega, q^2)/\partial\omega\partial q^2$. The latter turns out to be essential from the point of view of choosing optimum conditions for the experimental observation of complex singularities.

2. TRIANGULAR DIAGRAM. DIFFERENTIAL CROSS SECTION

The simplest mechanism for the reaction (1) is the quasielastic scattering of particle x by particle y which corresponds to a pole diagram. Such a mechanism yields a singularity with respect to the variable $(\mathbf{q} - \mathbf{p}_y)^2$ (\mathbf{p}_y is the momentum of particle y), but in this case there are no singularities with respect to the variables ω and q determined by the diagram itself. The simplest mechanism which leads to the appearance of such singularities corresponds to the triangular diagram shown

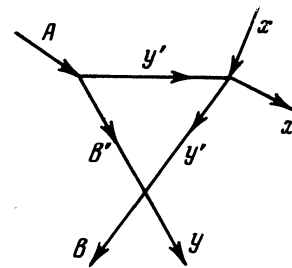


FIG. 1. The triangular diagram corresponding to the reaction $A + x \rightarrow B + x + y$.

in Fig. 1. According to this diagram the whole process reduces to three virtual reactions; to the decay of nucleus A into the virtual particles B' and y' .

$$A \rightarrow B' + y', \quad (2.1)$$

to the elastic virtual scattering of the incident particle x by particle y' ,

$$x + y' \rightarrow x + y', \quad (2.2)$$

and to the virtual reaction which leads to the production of final particles B and y

$$B' + y' \rightarrow B + y. \quad (2.3)$$

If $B' = B$ and $y' = y$, i.e., if the virtual reaction (2.3) is elastic scattering, then the diagram of Fig. 1 corresponds to taking into account the so-called final state interaction.

The triangular diagram of Fig. 1 corresponds to the amplitude (cf. ^[1])

$$M_{\Delta}(\omega, q) = -i(2\pi^4 \hbar)^{-1} m_{y'}^2 m_B \int \frac{M_A M_{xx} M_{y'y} d\mathbf{p}_{y'} dE_{y'}}{(p_{y'}^2 - 2m_{y'} E_{y'} - i0)(p_{y'}'^2 - 2m_{y'} E_{y'}' - i0)(p_B^2 - 2m_B E_B - i0)}. \quad (2.4)$$

Here (and in the rest of our discussion) m_i , E_i , \mathbf{p}_i denote respectively the mass, the kinetic energy and the momentum of the i -th particle; M_A , M_{xx} and $M_{y'y}$ are respectively the amplitudes for the virtual reactions (2.1), (2.2) and (2.3). All the amplitudes are rectangular matrices with respect to the spin indices, so that the numerator in the integrand should be interpreted as a product of rectangular matrices.

Each of the amplitudes M_A , M_{xx} , $M_{y'y}$ depends on the kinematic variables of the virtual particles. However, since we are interested in the behavior of the amplitude M_{Δ} near the singularity we can treat M_A , M_{xx} and $M_{y'y}$ as constants. Indeed, at the singularity $\omega = \omega_{\Delta}(q)$ the momenta of all the virtual particles lie on the mass surface and, therefore, are uniquely determined by the conservation laws and by the Landau conditions (cf., for example, ^[1], p. 39). From this it follows that the amplitudes for virtual processes for $\omega = \omega_{\Delta}(q)$ appear in M_{Δ} with completely determined values

of the kinematic variables, and if these values are not singularities of the amplitudes M_A , M_{xx} and $M_{y'y}$ then we are justified in taking these quantities outside the integral sign in (2.4) since the remainder of the integrand is a rapidly varying function near the singularity $\omega = \omega_{\Delta}(q)$. In this approximation the integral (2.4) can be evaluated, and the amplitude M_{Δ} will have the form

$$M_{\Delta}(\omega, q) = C f_{\Delta}(\omega, q), \quad (2.5)$$

where C is a rectangular matrix with respect to the spin indices of the initial (A, x) and final (B, y) particles which does not depend on ω and q :

$$C = -i \frac{(m_{y'})^2}{2\pi \hbar \kappa} \left(\frac{m_{B'}}{m_A} \right)^2 M_A M_{xx} M_{y'y}, \quad (2.6)$$

$$\kappa^2 = 2m_{B'y'}\varepsilon, \quad m_{B'y'} = \frac{m_{B'} m_{y'}}{m_{B'} + m_{y'}}, \quad (2.7)$$

$$\varepsilon = (m_{B'} + m_{y'} - m_A) c^2,$$

$$f_{\Delta} = \frac{-m_A \kappa}{m_{B'}} \frac{q}{q} \ln \frac{q_{\Delta} - iq}{q_{\Delta} + iq}, \quad (2.8)$$

$$q_{\Delta} = \frac{m_A}{m_{B'}} (\kappa + \sqrt{-p^2}), \quad (2.9)$$

$$p^2 = 2m_{B'y'}(\omega - Q) \quad Q = (m_{B'} + m_{y'} - m_B - m_y)c^2. \quad (2.10)$$

The function f_{Δ} has two singularities: a branch point involving a square root at $\omega = Q$ (the so-called normal threshold) and a logarithmic branch point. The motion of the singularity ω_{Δ} of the function f_{Δ} with respect to the variable ω depending on the variation of the transferred momentum q in the physical region ($q > 0$) is given by the equation

$$\frac{\omega_{\Delta}(q) - Q}{\epsilon} = \left(\frac{m_{B'}}{m_A}\right)^2 \frac{q^2}{\kappa^2} - 1 + 2i \frac{m_{B'}}{m_A} \frac{q}{\kappa}. \quad (2.11)$$

Similarly the motion of the singularity q_{Δ} of the function f_{Δ} with respect to the variable q depending on ω ($\omega - Q \geq 0$) is determined by the equation

$$\left(\frac{m_{B'}}{m_A}\right)^2 \frac{q_{\Delta}^2(\omega)}{\kappa^2} = \frac{\omega - Q}{\epsilon} - 1 + 2i \left(\frac{\omega - Q}{\epsilon}\right)^{1/2}. \quad (2.12)$$

The sheet of the square root in (2.9) is chosen so that the complex plane $z = -p^2$ is cut along the real negative semi-axis, while the sheet of the logarithm $\ln z$ is determined by the inequality

$$-\pi \leq \arg z < \pi.$$

As can be seen from (2.11) the degree of nearness of $\omega_{\Delta}(q)$ to the physical region is determined by the smallness of κ , i.e., by the smallness of the binding energy ϵ of particles B' and y' in nucleus A .

For subsequent discussion it will be convenient for us to go over to the dimensionless variables

$$\xi = \frac{\omega - Q}{\epsilon}, \quad \lambda = \frac{m_{B'}^2 q^2}{m_A^2 \kappa^2}. \quad (2.13)$$

Equations (2.11) and (2.12) for the motion of the logarithmic singularity then assumed the form

$$\lambda_{\Delta} = \xi - 1 + 2i\sqrt{\xi}, \quad \xi \geq 0, \quad (2.14)$$

$$\xi_{\Delta} = \lambda - 1 + 2i\sqrt{\lambda}, \quad \lambda \geq 0, \quad (2.15)$$

while the dimensionless amplitude f_{Δ} is given for real nonnegative values of λ by the equation

$$f_{\Delta}(\xi, \lambda) = \frac{1}{\sqrt{\lambda}} \left[\frac{1}{2} \ln \frac{(\sqrt{\xi} - \sqrt{\lambda})^2 + 1}{(\sqrt{\xi} + \sqrt{\lambda})^2 + 1} + i \operatorname{arctg} \frac{2\sqrt{\lambda}}{\xi - \lambda + 1} \right], \quad \xi \geq 0, \quad (2.16)^*$$

$$f_{\Delta}(\xi, \lambda) = \frac{2i}{\sqrt{\lambda}} \operatorname{arctg} \frac{\sqrt{\lambda}}{1 + \sqrt{-\xi}}, \quad \xi < 0. \quad (2.17)$$

Here we have $0 \leq \tan^{-1} < \pi$.

As has been already pointed out, contributions to the amplitude of reaction (1) are made, in addition to the triangular diagram considered above, also by other diagrams (in particular, the pole diagram). Therefore, the total amplitude for the reaction M should be written in the form

$$M = M_{\Delta} + M_R, \quad (2.18)$$

where we denote by M_R the contribution of all the other diagrams.

As a rule it is difficult to make a definite theoretical statement regarding the relative values of $|M_{\Delta}|$ and $|M_R|$, but it is possible to separate out the amplitude M_{Δ} near ω_{Δ} experimentally on the basis of the fact that in this region M_R must vary considerably more slowly than M_{Δ} , and can, therefore, be treated as a constant.

We obtain the differential cross section for the reaction by starting with the formula

$$d\sigma = \frac{1}{v} \frac{|M|^2}{(2\pi\hbar)^5} \delta(\epsilon_f - \epsilon_i) \delta(\mathbf{p}_f - \mathbf{p}_i) d\mathbf{p}_{x'} d\mathbf{p}_y d\mathbf{p}_{B_s} \quad (2.19)$$

where v is the relative velocity of the initial particles; $\epsilon_i, \epsilon_f, \mathbf{p}_i, \mathbf{p}_f$ are respectively the total energies and momenta of the initial and final states. After summing and averaging over the spins the differential cross section can be written as a function of the variables ξ and λ in the form

$$\partial^2 \sigma / \partial \xi \partial \lambda = N \sqrt{\xi} |f(\xi, \lambda)|^2. \quad (2.20)$$

Here

$$N = \frac{|C|^2}{16\pi^3 \hbar^5 v^2} \kappa^5 \frac{m_A^2 m_B^{3/2}}{(m_{B'})^{7/2}}, \quad (2.21)$$

$$|C|^2 = \frac{\operatorname{Sp} CC^+}{(2J_x + 1)(2J_A + 1)} \quad (2.22)$$

(J_x, J_A are the spins of particles x and A),

$$|f(\xi, \lambda)|^2 = |f_{\Delta}|^2 + 2a \operatorname{Re} f_{\Delta} + 2b \operatorname{Im} f_{\Delta} + c, \quad (2.23)$$

a, b, c are real constants:

$$a + ib = \frac{\operatorname{Sp} M_R C^+}{\operatorname{Sp} CC^+}, \quad c = \frac{\operatorname{Sp} M_R M_R^+}{\operatorname{Sp} CC^+}. \quad (2.24)$$

* $\operatorname{arctg} \equiv \tan^{-1}$.

The relation between the differential cross section $\partial^2\sigma/\partial\xi\partial\lambda$ and the differential cross section $\partial^2\sigma/E'_x dz$ is given in the laboratory system ($p_A = 0$) by the relation

$$\frac{\partial^2\sigma}{\partial E'_x \partial z} = \frac{m_x}{\sqrt{2}} \frac{m_B^{1/2} p_x p_{x'}}{m_y^{3/2} m_A \epsilon^2} \frac{\partial^2\sigma}{\partial \xi \partial \lambda}, \quad z = \frac{p_x p_{x'}}{p_x p_{x'}} \quad (2.25)$$

where E'_x is the kinetic energy of particle x after the reaction.

3. DISCUSSION OF THE RESULTS

As can be seen from formula (2.23) the dependence of the cross section on the variables ξ and λ is determined by an expression containing three unknown real constants. If C and the amplitude M_R do not depend on the orientation of the spins of the particles participating in the reaction, then the number of independent constants is equal to two (in this case $c = a^2 + b^2$). The constants a, b, and c must be determined from experimental data from the values of the differential cross section at three arbitrary points of the (ξ, λ) plane, and the resultant formula must then describe the whole surface $\partial^2\sigma/\partial\xi\partial\lambda$ (we emphasize that this means that the introduction of a maximum of three constant parameters permits the description of a large number of curves corresponding to different sections of the surface).

In order to visualize the degree of sharpness of the functional dependence determined by formula (2.23) it is useful to construct for each of the first three terms in (2.23) contour lines, i.e., curves in the (ξ, λ) plane along which the corresponding function of ξ and λ remains constant. It is not possible to obtain the equations for the contour lines of the surface $|f_\Delta(\lambda, \xi)|$ and $\text{Re } f_\Delta(\lambda, \xi)$, $\text{Im } f_\Delta(\xi, \lambda)$ in explicit form solved with respect to ξ or λ . However, it is possible to construct analytically a two parameter family of contour lines of the func-

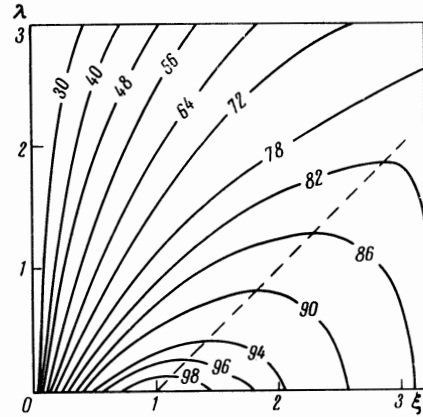


FIG. 3. Contour map of the surface $\text{Re } f_\Delta(\xi, \lambda)$. The numbers indicating the altitude of the contours are equal to $100 \text{Re } f_\Delta(\xi, \lambda)$.

tion $\lambda |f_\Delta(\xi, \lambda)|^2$. After performing on these latter contour lines a geometric transformation corresponding to the algebraic operation $1/\lambda$ we obtain contour lines of the surface $|f_\Delta(\xi, \lambda)|$ on the half-plane $\lambda \geq 0, -\infty < \xi < \infty$, which represent a surface monotonically decreasing as we move along any ray emerging from the point $\lambda = \xi = 0$. The curves of the contour lines of the surfaces $\text{Re } f_\Delta(\xi, \lambda)$, $\text{Im } f_\Delta(\xi, \lambda)$ also have negative curvature. The section of the surface $\text{Im } f_\Delta(\xi, \lambda)$ by the vertical plane along the straight line $\lambda = \text{const}$ has a single extremum (peak) at $\xi = 0$.

The contour lines of the surfaces $|f_\Delta|^2$ and $\text{Re } f_\Delta$ are given respectively in Figs. 2 and 3. The surface $\text{Im } f_\Delta$ is very close in its structure to the surface $|f_\Delta|$ (this is related to the fact that in the range of values under investigation the principal contribution to $|f_\Delta|$ is given by $\text{Im } f_\Delta$). From Figs. 2 and 3 it can be seen that the sections by the planes $\lambda = \text{const}$ or $\xi = \text{const}$ are by no means always the optimal ones for the discovery of functional relationships brought about by the complex singularity. In particular, if the dominant contribution to (2.23) is given by the terms $|f_\Delta|^2 + 2b \text{Im } f_\Delta$, then the most pronounced irregularity will appear if the section is made by a vertical plane along the straight line orthogonal to the line $\lambda = \xi + 1$ which is a projection of the trajectory of the complex singularity (2.15) on the (ξ, λ) plane. But if the dominant contribution is given by the term $a \text{Re } f_\Delta$ then the most prominent irregularity will appear if we take the section of the surface $\partial^2\sigma/\partial\xi\partial\lambda$ by the vertical plane along the straight line $\xi = \lambda + 1$ orthogonal to the projection of the complex singularity (2.14) on the (ξ, λ) plane. In all cases the dependence on the kinematic invariants q, ω is the more pronounced the smaller are the values of ϵ and κ . This circum-

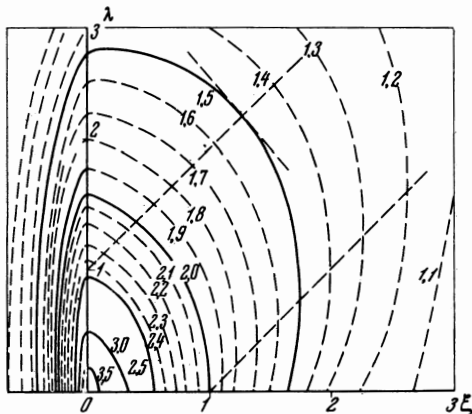


FIG. 2. Contour map of the surface $|f_\Delta(\xi, \lambda)|^2$.

stance is a consequence of the approach of the complex singularity (ω_Δ or q_Δ) to the $\text{Re } \omega$, $\text{Re } q$ plane on which the physical region is situated.

Another important factor which facilitates the experimental observation of the complex singularity is the greatest possible size of the physical region. The dimensions of the physical region are determined by the inequalities

$$4\xi_{Ax}\xi + (2\xi_{Ax} - \xi - \alpha\lambda - 1 + \xi_0)^2 \leq 4\xi_{Ax}(\xi_{Ax} - 1 + \xi_0), \quad (3.1)$$

$$\xi \geq \xi_0 = -Q/\epsilon, \quad \lambda \geq 0, \quad (3.2)$$

where ξ_{Ax} is the kinetic energy ω_{Ax} of the colliding particles A and x in their center of mass system expressed in units of ξ ($\xi_{Ax} = \omega_{Ax}/\epsilon$), and

$$\alpha = \frac{m_{y'} m_A + m_x}{m_x m_{B'}}. \quad (3.3)$$

The boundary of the physical region is the parabola whose symmetry axis makes an angle $\varphi = \tan^{-1} [m_x/(m_A + m_x)]$ with the ξ axis. The maximum value ξ_m of the variable ξ is given by the equation

$$\xi_m = \xi_{Ax} - 1 + \xi_0. \quad (3.4)$$

The value of λ corresponding to this point is

$$\lambda(\xi_m) = \alpha^{-1}\xi_{Ax}. \quad (3.5)$$

The minimum and the maximum values of λ corresponding to $\xi = \xi_0 = -Q/\epsilon$ are determined by the relation

$$\lambda = \alpha^{-1}(\sqrt{\xi_{Ax}} \pm \sqrt{\xi_{Ax} - 1})^2. \quad (3.6)$$

From formulas (3.4)–(3.6) it can be seen that the boundaries of the physical region spread out as the initial energy ξ_{Ax} is increased. In particular, for $\xi_{Ax} \gg 1$ the region of the most rapid variation of $\text{Re } f_\Delta$ determined by the complex singularity becomes accessible, while for

$$\xi_{Ax} \geq (\alpha + 1 - \xi_0)^2/4\alpha. \quad (3.7)$$

a segment of the straight line which is the projection of the trajectory (2.15) of the complex singularity, which we have mentioned before, is contained in the physical region.

We note that since for the majority of nuclei ϵ does not exceed 10 MeV energies of the order of 100 MeV in the center of mass system of the reaction are already sufficient for the experimental determination of the complex singularity corresponding to the diagram of Fig. 1.

We now investigate the manner in which the existence of a square root singularity at the point $\xi = 0$ affects the behavior of the cross section.

This point lies in the physical region only in the case when $\xi_0 \leq 0$, i.e., when the virtual reaction (2.3) is exothermic or when it represents elastic scattering. In the interval $\xi_0 \leq \xi \leq 0$ the expression for f_Δ is determined by Eq. (2.17). As can be easily seen on comparing (2.17) and (2.16), f_Δ is continuous at the point $\xi = 0$, while its first derivative has a discontinuity at that point:

$$f'_\Delta(\xi \rightarrow +0) = \frac{-1}{1+\lambda} \left[\frac{1}{\sqrt{\xi}} + \frac{2i}{1+\lambda} \right], \quad (3.8)$$

$$f'_\Delta(\xi \rightarrow -0) = \frac{i}{(1+\lambda)\sqrt{-\xi}}. \quad (3.9)$$

The discontinuity in the derivative will manifest itself in the differential cross section in the form of a characteristic peak^[6] (cf., also^[7]) which will be the sharper the smaller is the value of λ . Equations (3.8) and (3.9) show how the shape of the peak near $\xi = 0$ will change as the transferred momentum λ is varied. The curves corresponding to the section of the surface $\text{Im } f_\Delta$ and $\text{Re } f_\Delta$ by vertical planes $\lambda = \text{const}$ near $\xi = 0$ are shown respectively in Figs. 4 and 5. It should be noted that if the amplitude $|f(\xi, \lambda)|^2$ (cf. (2.23)) $|b| \gg a$ and $|b| \gg 1$, then the sign of the extrema will agree with the sign of b .

An example of a virtual reaction with $\xi_0 < 0$ is the process of inelastic scattering with “quenching” of excitation, i.e., the case when the virtual particle $B'(y')$ is an excited state of the final nucleus $B(y)$.

From the above discussion it follows that the possibility of identifying the mechanism of reaction (1) and, in particular, the elucidation of the role played by the final state interaction by means of an experimental investigation of the moving logarithmic and square-root branch points of the amplitude corresponding to the diagram of Fig. 1 appears to be quite real for a sufficiently high energy of the incident particles (of the order of several tens of MeV in the center of mass system for the reaction).

In conclusion we note the relation between the approximations utilized in the present paper and the well known results of Watson^[8] and Migdal^[9] based on taking the final state interaction into account. As has been noted earlier (Sec. 2) our basic assumption was the nearness to the singularity and the relatively slow variation at that point of the amplitudes of the virtual processes. In contrast to this, Watson and Migdal consider the case when the dependence of the amplitude on the kinematic variables due to the mechanism of the reaction itself is weak compared to the variation in the ampli-

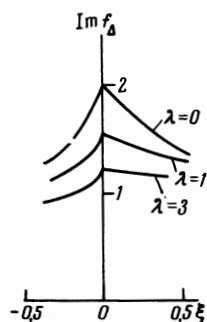


FIG. 4. The shape of the curves corresponding to the vertical sections of the surface $\text{Im } f_{\Delta}(\xi, \lambda)$ by the planes $\lambda = \text{const}$ near the square root singularity $\xi = 0$.

tude of virtual scattering as a function of ω . One can give examples of processes in which dependences of both these types are significant—such an example is the reaction $p + d \rightarrow 2p + n$ which is as yet the only example of a sufficiently complete experimental study of the surface $\partial^2 \sigma / \partial \xi \partial \lambda$ ^[10] (the amplitude of p-n scattering turns out in this case to be a noticeably varying function for small values of ω due to the presence of a virtual singlet pole). A theoretical analysis can also be carried out for this reaction—the corresponding triangular diagram has been evaluated by Komarov and Popova.^[11]

The domain of applicability of the results obtained above is limited, firstly, by the assumption regarding the approximate constancy of the amplitudes of the virtual processes and, secondly, by the neglect of the Coulomb interaction if both final particles are charged. The latter can primarily affect the behavior near the threshold singularity, but can be easily taken into account in that case. Concerning the variation of the amplitudes of virtual processes one can say that except for individual reactions of the type of the break-up of a deuteron by nucleons mentioned above it is difficult to obtain reliable theoretical estimates since we are dealing with the behavior of amplitudes in nonphysical regions. This question can be elucidated only by a comparison of experimental data with theoretical results obtained on the assumption that the virtual amplitudes are constant near the singularities of the diagram.

Finally, we note that the results obtained in this paper can be generalized to reactions involving the

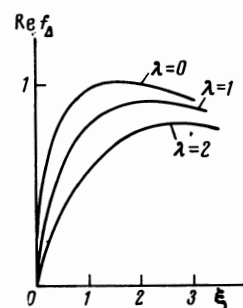


FIG. 5. The shape of the curves corresponding to the vertical sections of the surface $\text{Re } f_{\Delta}$ by the planes $\lambda = \text{const}$.

production of three particles of arbitrary type, i.e., processes $A + x \rightarrow B + y + z$.

The authors express their gratitude to E. Baranova for her aid with numerical computations.

¹ I. S. Shapiro, *Teoriya pryamykh yadernykh reaktsii* (Theory of Direct Nuclear Reactions), Gosatomizdat, 1963.

² L. D. Blokhintsev, E. I. Dolinskiĭ and V. S. Popov, *JETP* **43**, 2291 (1962), *Soviet Phys. JETP* **16**, 1618 (1963).

³ V. N. Valuev, *JETP* **47**, 649 (1964), *Soviet Phys. JETP* **20**, 433 (1965).

⁴ V. V. Anisovich and L. G. Dakhno, *JETP* **46**, 1153 (1964), *Soviet Phys. JETP* **19**, 779 (1964).

⁵ O. D. Dal'karov, *JETP Letters* **3**, 150 (1966), transl., p. 94.

⁶ A. I. Baz', *JETP* **33**, 923 (1957), *Soviet Phys. JETP* **6**, 709 (1958).

⁷ L. D. Landau and E. M. Lifshitz, *Kvantovaya mekhanika* (Quantum Mechanics), Fizmatgiz, 1963, p. 653.

⁸ K. M. Watson, *Phys. Rev.* **88**, 1163 (1952).

⁹ A. B. Migdal, *JETP* **28**, 3 (1955), *Soviet Phys. JETP* **1**, 2 (1955).

¹⁰ W. D. Sympton et al., *Revs. Modern Phys.* **37**, 523 (1965).

¹¹ V. V. Komarov and A. M. Popova, *Nucl. Phys.* **54**, 278 (1964).

Translated by G. Volkoff